Article

Low-temperature formation of pyridine and (iso)quinoline via neutral–neutral reactions

In the format provided by the authors and unedited

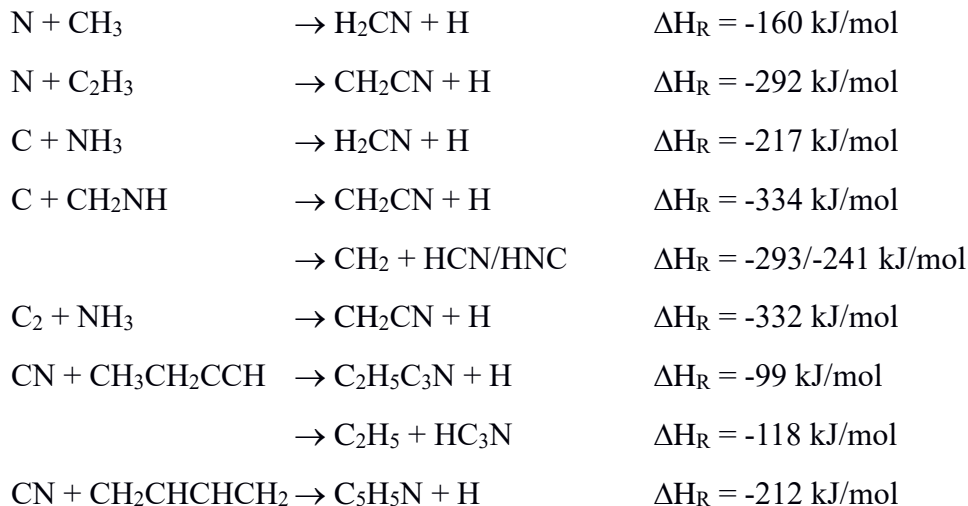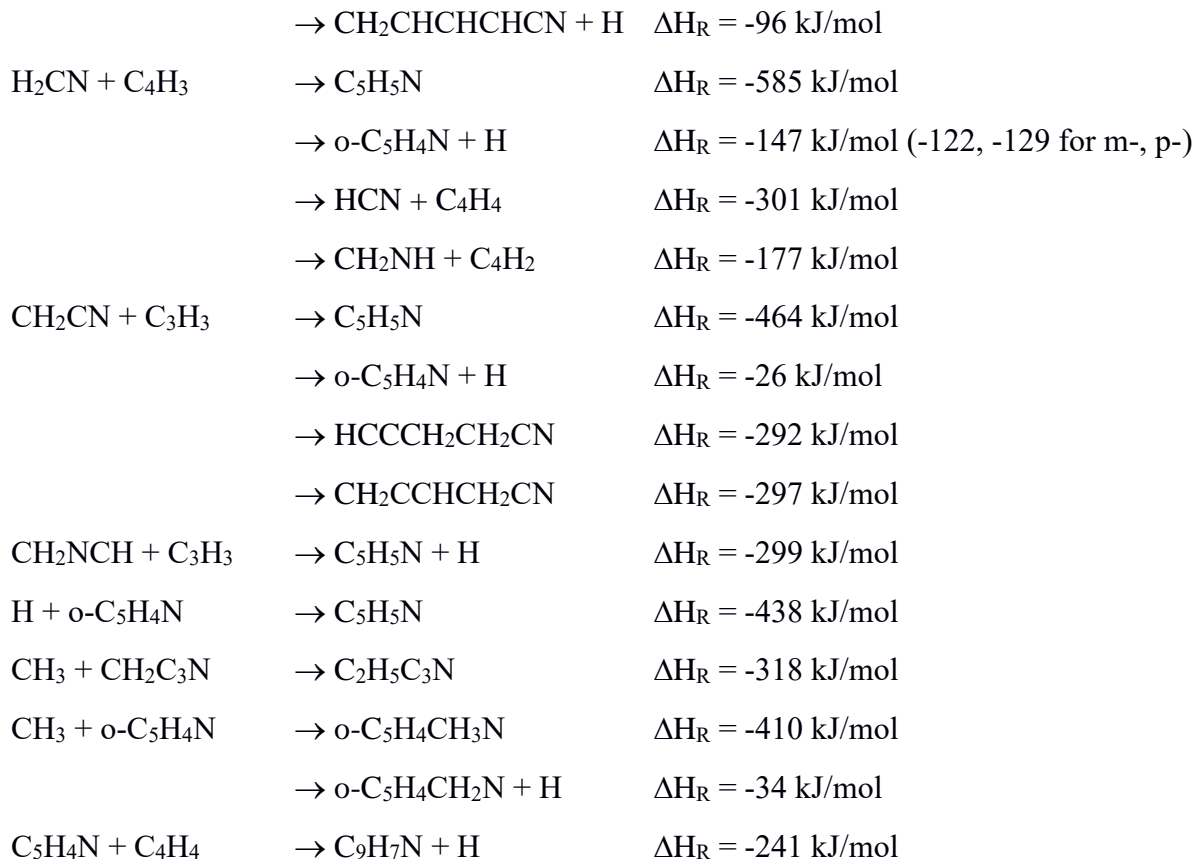**Supplementary Note 1: Suprathermal hydrogen-atom assisted isomerization**

Althuogh RRKM results predict that **p1** only contributes around 8% at the low temperature conditions of TMC-1 and Titan, the experimental results might be explained by the suprathermal hydrogen-atom assisted isomerization mechanism (Supplementary Tables 2-3). Suprathermal hydrogen atoms with excess kinetic energies of a few electron volts can be formed via photodissociation of hydrides like methane (CH_4) by solar photons, via neutral-neutral reactions of, e.g., methylidyne (CH) with methane, and/or electron recombination reactions of with abundant ions (CH_5^+, CH_3^+, and $C_6H_7^+$)[1-3]. These suprathermal hydrogen atoms are not in thermal equilibrium with the surrounding low-temperature atmosphere and their kinetic energies can easily exceed 100 kJ mol^{-1} (1.04 eV)[1,4]. The rapid suprathermal hydrogen-atom assisted isomerization processes of converting the high-energy isomers **p3** and **p4** to **p1** are very efficient due to absence of a barrier of **p4 + H → i2** and a small barrier of only 20 kJmol^{-1} for **p3 + H → i3**[5,6]. As depicted in Supplementary Fig. 3-4, the elevated rate constants of **p3** + H of a few 10^{-10} cm^{3}s^{-1} can be reached with suprathermal hydrogen atoms possessing high kinetic energies.

Supplementary Note 2: Results of the astrochemical modeling of Titan's atmosphere

The main aspects of the chemistry of the formation of pyridine (C_5H_5N) and ethylcyanoacetylene ($C_2H_5C_3N$) (the most abundant linear C_5H_5N isomer deduced from production fluxes) and (iso)quinoline (C_9H_7N) are presented below[7-11]:

$N + CH_3$	$\rightarrow H_2CN + H$	$\Delta H_R = -160$ kJ/mol
$N + C_2H_3$	$\rightarrow CH_2CN + H$	$\Delta H_R = -292$ kJ/mol
$C + NH_3$	$\rightarrow H_2CN + H$	$\Delta H_R = -217$ kJ/mol
$C + CH_2NH$	$\rightarrow CH_2CN + H$	$\Delta H_R = -334$ kJ/mol
	$\rightarrow CH_2 + HCN/HNC$	$\Delta H_R = -293/-241$ kJ/mol
$C_2 + NH_3$	$\rightarrow CH_2CN + H$	$\Delta H_R = -332$ kJ/mol
$CN + CH_3CH_2CCH$	$\rightarrow C_2H_5C_3N + H$	$\Delta H_R = -99$ kJ/mol
	$\rightarrow C_2H_5 + HC_3N$	$\Delta H_R = -118$ kJ/mol
$CN + CH_2CHCHCH_2$	$\rightarrow C_5H_5N + H$	$\Delta H_R = -212$ kJ/mol

	$\rightarrow$ CH$_2$CHCHCHCN + H	ΔH_R = -96 kJ/mol
H$_2$CN + C$_4$H$_3$	$\rightarrow$ C$_5$H$_5$N	ΔH_R = -585 kJ/mol
	$\rightarrow$ o-C$_5$H$_4$N + H	ΔH_R = -147 kJ/mol (-122, -129 for m-, p-)
	$\rightarrow$ HCN + C$_4$H$_4$	ΔH_R = -301 kJ/mol
	$\rightarrow$ CH$_2$NH + C$_4$H$_2$	ΔH_R = -177 kJ/mol
CH$_2$CN + C$_3$H$_3$	$\rightarrow$ C$_5$H$_5$N	ΔH_R = -464 kJ/mol
	$\rightarrow$ o-C$_5$H$_4$N + H	ΔH_R = -26 kJ/mol
	$\rightarrow$ HCCCH$_2$CH$_2$CN	ΔH_R = -292 kJ/mol
	$\rightarrow$ CH$_2$CCHCH$_2$CN	ΔH_R = -297 kJ/mol
CH$_2$NCH + C$_3$H$_3$	$\rightarrow$ C$_5$H$_5$N + H	ΔH_R = -299 kJ/mol
H + o-C$_5$H$_4$N	$\rightarrow$ C$_5$H$_5$N	ΔH_R = -438 kJ/mol
CH$_3$ + CH$_2$C$_3$N	$\rightarrow$ C$_2$H$_5$C$_3$N	ΔH_R = -318 kJ/mol
CH$_3$ + o-C$_5$H$_4$N	$\rightarrow$ o-C$_5$H$_4$CH$_3$N	ΔH_R = -410 kJ/mol
	$\rightarrow$ o-C$_5$H$_4$CH$_2$N + H	ΔH_R = -34 kJ/mol
C$_5$H$_4$N + C$_4$H$_4$	$\rightarrow$ C$_9$H$_7$N + H	ΔH_R = -241 kJ/mol

The rates of these barrier-free reactions are incorporated from capture theory when no experimental measurements exist, while the rates of the three-body reactions are taken to be equal to similar reactions of benzene derivatives. For some reactions such as CN + CH$_2$CHCHCH$_2$ (and also CH$_2$CN + C$_3$H$_3$) the formation of pyridine is in competition with the formation of nitriles, see for example[7,10]. The destruction of pyridine, C$_2$H$_5$C$_3$N and quinoline occurs mainly through photodissociation, through reactions with N(^{2}D)[12] and C$_2$H, and through reactions with ions such as HCNH$^+$, C$_2$H$_5^+$, NH$_4^+$. Unlike benzene where ionic chemistry plays an important role in its formation through the C$_4$H$_3^+$ + C$_2$H$_2$ and C$_4$H$_3^+$ + C$_2$H$_4$ reactions[13,14], ionic reactions do not appear to be effective in producing pyridine (nor likely quinoline). Indeed the pyridine forming reaction C$_4$H$_3^+$ + HCN is slow, in contrast to the benzene forming reaction C$_4$H$_3^+$ + C$_2$H$_2$[15], and even if the reaction C$_4$H$_3^+$ + CH$_2$NH is fast (this reaction has never been studied to the best of our knowledge) the flux will be much smaller than the reaction C$_4$H$_3^+$ + C$_2$H$_4$ because CH$_2$NH is much less abundant than C$_2$H$_4$ (CH$_2$NH has not yet been detected in Titan's atmosphere). Moreover, the proton affinity of pyridine (937 kJ mol^{-1}) is very high which will induce a proton transfer from ions (HCNH$^+$, C$_2$H$_5^+$, NH$_4^+$ and so on) to C$_5$H$_5$N. If the electronic recombination reaction of

$C_5H_5NH^+$ does not lead to a 100% yield of $C_5H_5N + H$, not only will the ionic chemistry not induce the formation of pyridine, but it will promote its destruction instead.

The absorption spectrum of pyridine and quinoline and the products for the photodissociation of pyridine has been studied. The products for the photodissociation of quinoline are deduced from photodissociation of similar species[16-19]. For pyridine (and quinoline) photodissociation, the rate we use is in fact the maximum limit. Indeed, as for benzene, the lifetime of $C_5H_5N^{**}$ produced after photon absorption is quite long so some of these molecules will stabilize before dissociating[19]. On the other hand, the lifetime of pyridine is shorter than benzene (the pyridine lifetime is 0.1 μs following excitation at 193 nm compared with 10 μs for benzene) so photodissociation will be more efficient for pyridine than for benzene. The absorption of $C_2H_5C_3N$ has not been studied to the best of our knowledge but the photodissociation of this species will be dominated by the absorption of the chromophore $-C_3N$, so its absorption spectrum is taken to be the same as CH_3C_3N. The photodissociation products of $C_2H_5C_3N$ are assumed to be $C_2H_4 + HC_3N$ and $CH_3 + CH_2C_3N$.

To evaluate the uncertainties on the nominal model profiles, obtained using the recommended rate constants, a Monte Carlo simulation was performed according to the method described in Benne et al.[20]. Briefly, the rate constants for all reactions were recalculated using their associated uncertainty factors, F_i, the temperature-dependent uncertainty factor, and g_i, a coefficient used to extrapolate F_i to lower temperature, allowing $F_i(T)$ to be determined. Each rate constant was considered to be a random variable, k_i, with a log-normal distribution centered on the nominal value, k_{0_i}, with a standard deviation, $\log F_i$. For bimolecular reactions, k_i was given by

$$\log(k_i) = \log(k_{0_i}) + \varepsilon_i \log[F_i(T)]$$

As ε_i is a random number with a normal distribution centered on zero and a standard deviation of one, this led to a 68.3 % probability of finding a k_i value within the interval $\left[\frac{k_{0_i}}{F_i}, k_{0_i} \times F_i\right]$. 280 simulations were performed using this procedure to establish the possible dispersion from the nominal mole fraction profiles displayed in Figure 5.

The mole fraction of ammonia (NH_3) in Titan's atmosphere is still a tricky question. Ammonia abundances have been inferred indirectly via the Cassini's Ion and Neutral Mass Spectrometer (INMS) detection of the ammonium cation (NH_4^+) predicting high mole fraction of ammonia of $(3\text{-}4)\times10^{-5}$ at around 1000 km[21]. However, photochemical models cannot replicate these findings and underestimate mole fractions by up to two orders of magnitude[22,23]. In the stratosphere, the

calculated ammonia mole fraction is consistent with upper limits derived from Composite Infrared Spectrometer (CIRS) and Herschel[23,24]. These photochemical models reveal that two C_5H_5N isomers, pyridine (C_5H_5N) and ethylcyanoacetylene (C_2H_5CCCN), display significant mole fractions of 1.4×10^{-7} and 2.3×10^{-7} in the ionosphere of Titan, respectively. The maximum mole fraction for (iso)quinoline is predicted to be 1.7×10^{-11} around 1,100 km, which should be observable spectroscopically. These models also predict maximum mole fractions of $C_5H_5NH^+$ and $C_2H_5C_3NH^+$ of 1.5×10^{-10} and 3.9×10^{-10} at around 1,100 km, respectively. Accounting for the uncertainties, the mole fraction of $(1.5 \pm 0.3) \times 10^{-9}$ at m/z = 80 ($C_5H_5NH^+$) derived from the Cassini INMS data[25,26] agrees within the error limits well with the sum of mole fractions of $C_5H_5NH^+$ and $C_2H_5C_3NH^+$ of the atmospheric models ranging between 2.5×10^{-9} to 5.4×10^{-10}.

Supplementary Note 3: Additional PES results

Three distinct entrance channels lead barrierlessly to **i1''** to **i3''**. Extensive hydrogen shifts, and cyclization accompanied by aromatization to pyridine (C_5H_5N, **i12''**), which undergoes three barrierless hydrogen loss pathways to distinct pyridinyl radicals. It is interesting to point out that analogous barrierless pathways are identified in the cis-HCNH-$C_4H_3^\bullet$ system, in which two distinct entrance channels lead barrierlessly to **i14''** and **i19''** followed by hydrogen shifts and cyclization to pyridine and pyridinyl radicals. Overall, we depict evidence that in Titan's atmosphere, where abundant suprathermal hydrogen atoms exist, **p3** can efficiently undergo suprathermal hydrogen atom − assisted isomerization to **p1**, the most stable isomer, followed by the reactions with i/n-C_4H_3 isomers to pyridine and pyridinyl radicals. Even **p3** itself can itself react with i/n-C_4H_3 isomers barrierlessly leading to pyridine and pyridinyl radicals (Extended Data Figs. 2-3).

Supplementary Note 4: Results of the astrochemical modeling of TMC-1

The low temperature chemical mass growth processes in cold molecular clouds such as TMC-1 is fundamentally distinct from those in atmospheres of planets and their moons with both interstellar (TMC-1) and solar system (Titan) low-temperature environments require the absence of any entrance barriers to overall exoergic reactions[27]. However, the low number densities of molecules in molecular clouds ranging from 10^4 to 10^6 cm^{-3} necessitate bimolecular reactions; third body collisions, in which collisions of the reaction intermediate with a bath molecule divert the internal energy of the intermediate and hence stabilize the latter, are absent. This requires

changes to the reaction network from Titan's atmosphere (Figure 1) to TMC-1 thus implementing a reaction network of barrierless and exoergic bimolecular reactions (Supplementary Fig. 5, (Supplementary Table 4) such as reactions (1) and (2). Physical parameters were modernized according to Markwick et al.[28], McElroy et al.[29], and Yang et al.[30] with a temperature of 10 K, a cosmic ray ionization rate of 1.3×10^{-17} s^{-1}, a visual extinction of 10 Mag, and a number density of molecular hydrogen of 10^4 cm^{-3}. The carbon – ammonia system can account for 30 % to 75 % of the observed methylene amidogen radicals; generally spoken, as the initial abundances of nitrogen increase or carbon decreases, the fraction of methylene amidogen rises. For example, the contribution from the carbon – ammonia system rises to 50 % when the fraction of nitrogen increases to 10^{-2} and even to 75 % with at a fraction of 10^{-1}; these cases operate in those regions of TMC-1 where nitrogen-rich species are injected into the gas phase from the icy grains[31,32]. Model outputs of the closed shell nitriles vinyl cyanide (C_2H_3CN) and methyl cyanide (CH_3CN) are reported to be $(8.6 \pm 0.6) \times 10^{-10}$ after 3.2×10^5 year and $(1.0 \pm 0.2) \times 10^{-9}$ after 2.5×10^5 years also close to the observed data with important routes of barrierless reactions of the cyano radical (CN) with ethylene (C_2H_4)[33] and of the vinyl radical (C_2H_3) with the imidogen radical (NH)[34].
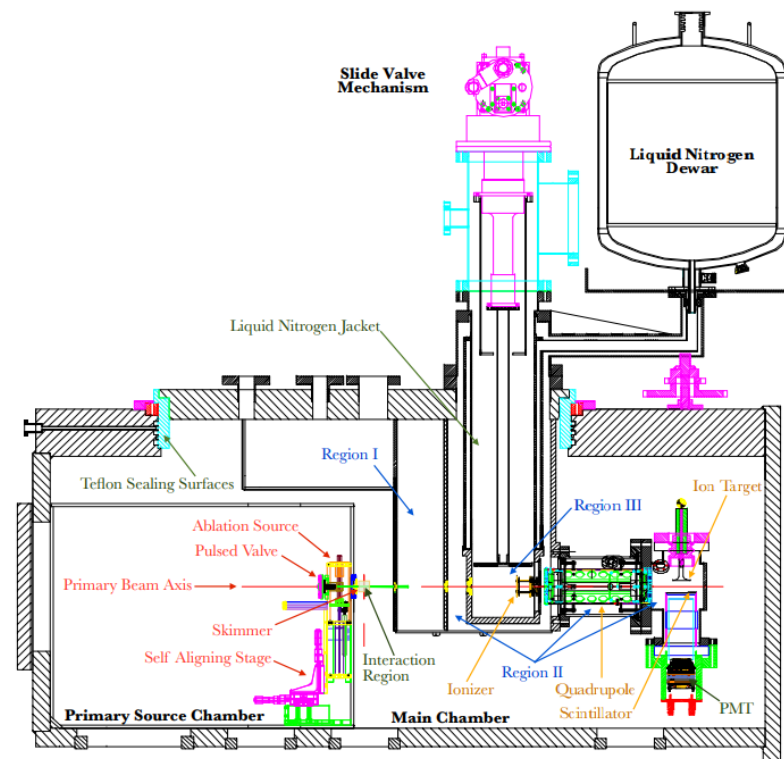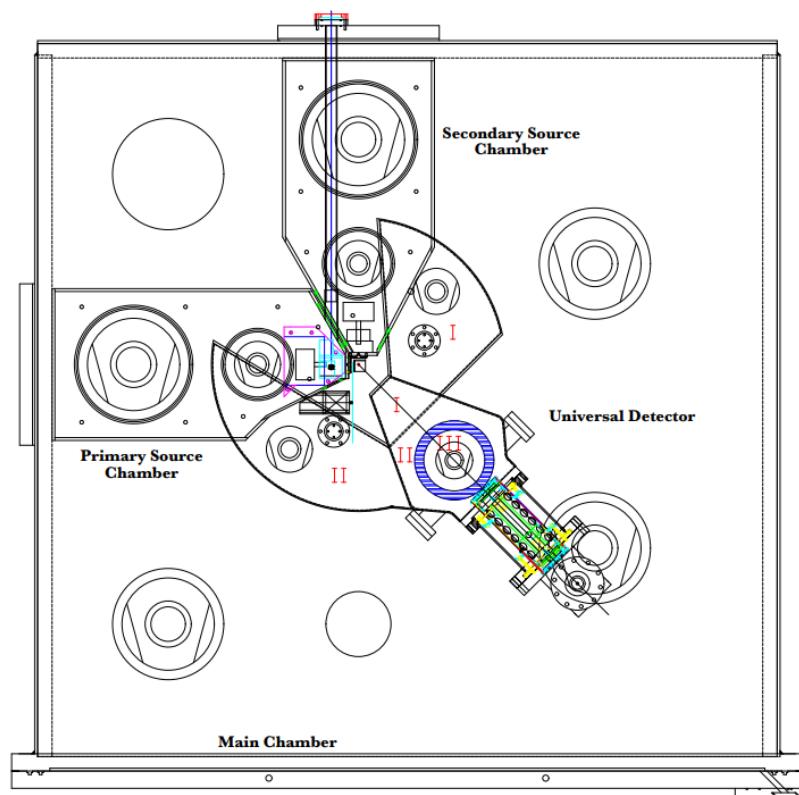
Supplementary Fig. 1. **Schematic of the crossed molecular beam machine.** The QMS is operated in time-of-flight mode and the flight time of a product molecule at a well defined mass-to-charge ratio from the interaction region to the ionizer is collected during the experiment.
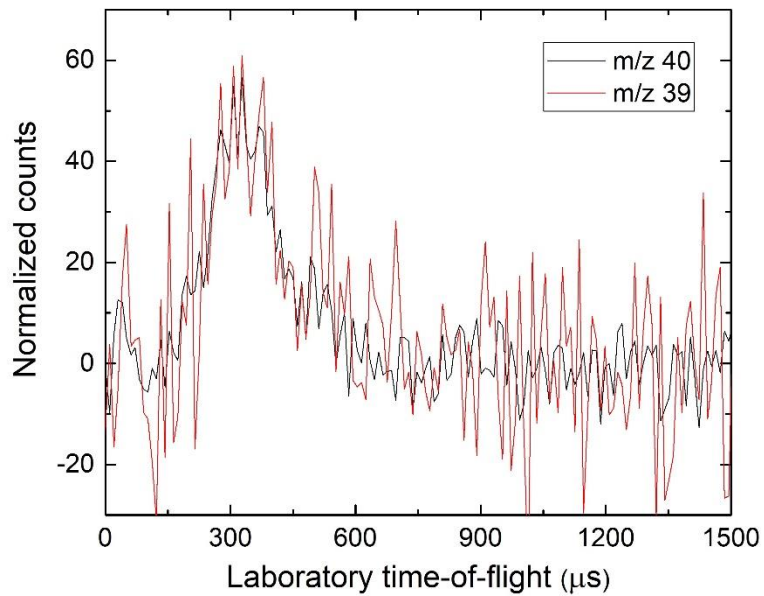
Supplementary Fig. 2. **Scaled time-of-flight spectra.** Mass spectra recorded at the CM angles for m/z = 40 and 39 for the C_2-NH_3 reaction are indistinguishable after scaling.
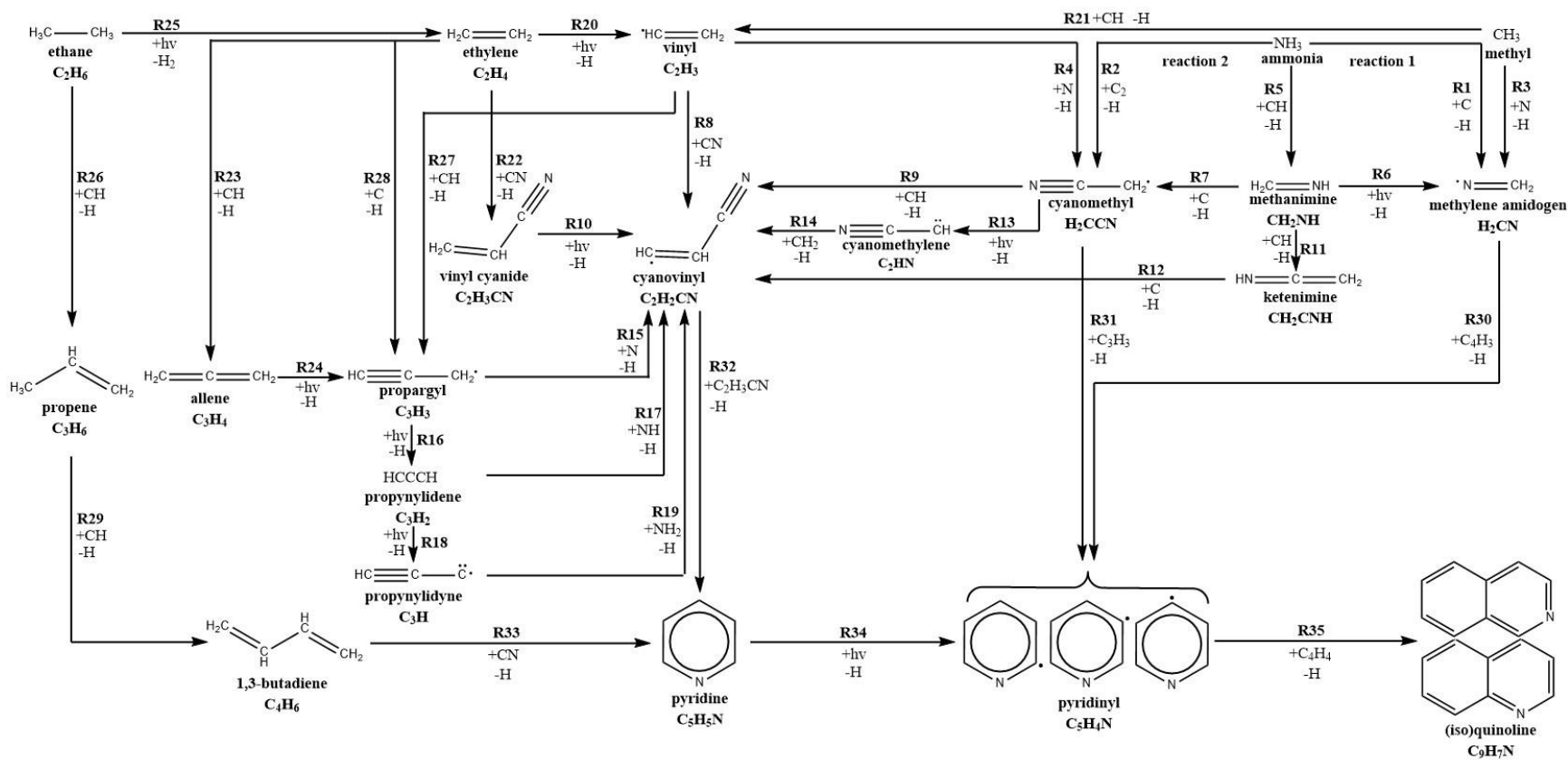
1
2 **Supplementary Fig. 3**. **Updated reaction network in TMC-1.** Compilation of key bimolecular reactions and photodissociation
3 processes newly introduced into the astrochemical model for TMC-1 leading to pyridine, pyridinyl, and (iso)quinoline.

Supplementary Table 1. Peak velocity (v_p) and speed ratios (S) of the atomic carbon (C; ^{3}P), dicarbon (C_2; $X^1\Sigma_g^+/a^3\Pi_u$), ammonia (NH_3; X^1A_1), and D3-ammonia (ND_3; X^1A_1) beams along with the corresponding collision energy (E_C) and center-of-mass angle (Θ_{CM}) for each reactive scattering experiment.

beam	v_p (m s^{-1})	S	E_c (kJ mol^{-1})	Θ_{CM} (deg)
C	2512 ± 49	2.9 ± 0.3		
ND_3	1091 ± 25	10.1 ± 1.3	28.1 ± 0.9	35.9 ± 0.5
C_2	1451 ± 19	3.2 ± 0.1		
NH_3	1143 ± 34	10.3 ± 1.4	17.0 ± 0.3	29.2 ± 0.3

Supplementary Table 2. Statistical branching ratios (%) for the reaction of carbon with D3-ammonia (ND_3) at the collision energies (E_c, kJ mol^{-1}) of 0 and 28.1 kJ mol^{-1}.

E_c	**p1**	**p2**	**p3**	**p4**
0	8	41	33	18
28.1	7	33	29	31

Supplementary Table 3. The RRKM rate constants (s^{-1}) for the C-ND$_3$ reaction computed at collision energies of 0.0 and 28.1 kJ mol^{-1}.

	0.0	28.1
(i1 →i2)	5.27×10^{10}	4.13×10^{11}
(i2 →i1)	3.70×10^{7}	5.36×10^{8}
(i1 →p4)	8.09×10^{9}	1.37×10^{11}
(i2 →i3)	1.56×10^{11}	2.73×10^{11}
(i3 →i2)	1.13×10^{11}	2.01×10^{11}
(i2 →p2)	5.35×10^{11}	9.16×10^{11}
(i2 →p3)	4.36×10^{11}	8.12×10^{11}
(i2 →p4)	6.41×10^{10}	1.64×10^{11}
(i3 →i4)	5.84×10^{11}	8.16×10^{11}
(i4 →i3)	1.64×10^{12}	2.48×10^{12}
(i3 →p1)	3.24×10^{12}	4.45×10^{12}
(i3 →p2)	7.71×10^{11}	1.26×10^{12}
(i3 →p3)	4.60×10^{11}	8.50×10^{11}
(i4 →p1)	2.12×10^{13}	2.98×10^{13}

Supplementary Table 4. Key bimolecular reactions and photodissociation processes associated with the $C/C_2 - NH_3$ systems newly incorporated into the astrochemical model.

Reactant 1	Reactant 2	Products	α	β	γ	No.
NH_3	C	H_2CN+H	4.00E-10	0	0	R1
NH_3	C_2	CH_2CN+H	4.00E-10	0	0	R2
CH_3	N	H_2CN+H	4.00E-10	0	0	R3
C_2H_3	N	CH_2CN+H	4.00E-10	0	0	R4
NH_3	CH	CH_2NH+H	4.00E-10	0	0	R5
CH_2NH	hv	H_2CN+H	3.00E-09	0	3.1	R6
CH_2NH	C	CH_2CN+H	4.00E-10	0	0	R7
C_2H_3	CN	C_2H_2CN+H	4.00E-10	0	0	R8
CH_2CN	CH	C_2H_2CN+H	4.00E-10	0	0	R9
C_2H_3CN	hv	C_2H_2CN+H	3.00E-09	0	3.1	R10
CH_2NH	CH	CH_2CNH+H	4.00E-10	0	0	R11
CH_2CNH	C	C_2H_2CN+H	4.00E-10	0	0	R12
CH_2CN	hv	C_2HN+H	3.00E-09	0	3.1	R13
C_2HN	CH_2	C_2H_2CN+H	4.00E-10	0	0	R14
C_3H_3	N	C_2H_2CN+H	4.00E-10	0	0	R15
C_3H_3	hv	C_3H_2+H	3.00E-09	0	3.1	R16
C_3H_2	NH	C_2H_2CN+H	4.00E-10	0	0	R17
C_3H_2	hv	C_3H+H	3.00E-09	0	3.1	R18
C_3H	NH_2	C_2H_2CN+H	4.00E-10	0	0	R19
C_2H_4	hv	C_2H_3+H	3.00E-09	0	3.1	R20
CH_3	CH	C_2H_3+H	4.00E-10	0	0	R21
C_2H_4	CN	C_2H_3CN+H	4.00E-10	0	0	R22
C_2H_4	CH	C_3H_4+H	4.00E-10	0	0	R23
C_3H_4	hv	C_3H_3+H	3.00E-09	0	3.1	R24
C_2H_6	hv	$C_2H_4+H_2$	3.00E-09	0	3.1	R25
C_2H_6	CH	C_3H_6+H	4.00E-10	0	0	R26
C_2H_3	CH	C_3H_3+H	4.00E-10	0	0	R27
C_2H_4	C	C_3H_3+H	4.00E-10	0	0	R28
C_3H_6	CH	C_4H_6+H	4.00E-10	0	0	R29
H_2CN	C_4H_3	C_5H_4N+H	4.00E-10	0	0	R30
CH_2CN	C_3H_3	C_5H_4N+H	4.00E-10	0	0	R31
C_2H_2CN	C_2H_3CN	C_5H_5N+CN	4.00E-10	0	0	R32
C_4H_6	CN	C_5H_5N+H	4.00E-12	0	0	R33
C_5H_5N	hv	C_5H_4N+H	3.00E-09	0	3.1	R34
C_5H_4N	C_4H_4	C_9H_7N+H	4.00E-10	0	0	R35
CH_3CN	hv	CH_2CN+H	3.00E-09	0	3.1	R36
C_2H_3	NH	CH_3CN+H	4.00E-10	0	0	R37
CN	CH_3	CH_2CN+H	4.00E-10	0	0	R38
C_2H	NH_2	CH_2CN+H	4.00E-10	0	0	R39
C_2H_3	hv	C_2H_2+H	3.00E-09	0	3.1	R40
C_2H_4	hv	$C_2H_2+H_2$	3.00E-09	0	3.1	R41
CH_3	C	C_2H_2+H	4.00E-10	0	0	R42
CH_2	CH	C_2H_2+H	4.00E-10	0	0	R43
CH_2	NH	H_2CN+H	4.00E-10	0	0	R44
CH	NH_2	H_2CN+H	4.00E-10	0	0	R45
CH_3	NH	CH_2NH+H	4.00E-10	0	0	R46
CH_2	NH_2	CH_2NH+H	4.00E-10	0	0	R47
C_4H_5N	CH	C_5H_5N+H	4.00E-10	0	0	R48
C_3H_6	CN	C_4H_5N+H	4.00E-10	0	0	R49
CH_3CN	C	C_2H_2CN+H	4.00E-10	0	0	R50

Supplementary References

1   Morton, R. J. & Kaiser, R. I. Kinetics of suprathermal hydrogen atom reactions with saturated hydrides in planetary and satellite atmospheres. *Planet. Space Sci.* **51**, 365-373 (2003).

2   De La Haye, V., Waite, J. H., Cravens, T. E., Robertson, I. P. & Lebonnois, S. Coupled ion and neutral rotating model of Titan's upper atmosphere. *Icarus* **197**, 110-136 (2008).

3   Vuitton, V., Yelle, R. V., Klippenstein, S. J., Hörst, S. M. & Lavvas, P. Simulating the density of organic species in the atmosphere of Titan with a coupled ion-neutral photochemical model. *Icarus* **324**, 120-197 (2019).

4   De La Haye, V. *et al.* Heating Titan's upper atmosphere. *J. Geophys. Res.* **113** (2008).

5   Mebel, A. M., Georgievskii, Y., Jasper, A. W. & Klippenstein, S. J. Pressure-dependent rate constants for PAH growth: formation of indene and its conversion to naphthalene. *Faraday Discuss.* **195**, 637-670 (2016).

6   Jasper, A. W. & Hansen, N. Hydrogen-assisted isomerizations of fulvene to benzene and of larger cyclic aromatic hydrocarbons. *Proc. Combust. Inst.* **34**, 279-287 (2013).

7   Sun, B. J. *et al.* Theoretical study on reaction mechanism of ground-state cyano radical with 1, 3-butadiene: prospect of pyridine formation. *J. Phys. Chem. A* **118**, 7715-7724 (2014).

8   Parker, D. S. N. *et al.* On the formation of pyridine in the interstellar medium. *Phys. Chem. Chem. Phys.* **17**, 32000-32008 (2015).

9   Parker, D. S. N. & Kaiser, R. I. On the formation of nitrogen-substituted polycyclic aromatic hydrocarbons (NPAHs) in circumstellar and interstellar environments. *Chem. Soc. Rev.* **46**, 452-463 (2017).

10   Morales, S. B. *et al.* A crossed molecular beam, low-temperature kinetics, and theoretical investigation of the reaction of the cyano radical (CN) with 1, 3-butadiene (C_4H_6). A route to complex ritrogen-bearing molecules in low-temperature extraterrestrial environments. *Astrophys. J.* **742**, 26 (2011).

11   Loison, J. C. *et al.* The neutral photochemistry of nitriles, amines and imines in the atmosphere of Titan. *Icarus* **247**, 218-247 (2015).

12   Recio, P. *et al.* A crossed molecular beam investigation of the $N(^2D)$ + pyridine reaction and implications for prebiotic chemistry. *Chem. Phys. Lett.* **779**, 138852 (2021).

13   Loison, J. C., Dobrijevic, M. & Hickson, K. M. The photochemical production of aromatics in the atmosphere of Titan. *Icarus* **329**, 55-71 (2019).

14   Vuitton, V., Yelle, R. V. & Cui, J. Formation and distribution of benzene on Titan. *J. Geophys. Res.* **113** (2008).

15   Anicich, V. G. An index of the literature for bimolecular gas phase cation-molecule reaction kinetics. (2003).

16   Bolovinos, A., Tsekeris, P., Philis, J., Pantos, E. & Andritsopoulos, G. Absolute vacuum ultraviolet absorption spectra of some gaseous azabenzenes. *J. Mol. Spectrosc.* **103**, 240-256 (1984).

17   Leach, S., Jones, N. C., Hoffmann, S. V. & Un, S. VUV Absorption Spectra of Gas-Phase Quinoline in the 3.5–10.7 eV Photon Energy Range. *J. Phys. Chem. A* **122**, 5832-5847 (2018).

18   Prather, K. A. & Lee, Y. T. The Photodissociation of Pyridine at 193 nm. *Israel journal of chemistry* **34**, 43-53 (1994).

19   Lin, M.-F. *et al.* Photodissociation dynamics of pyridine. *J. Chem. Phys.* **123**, 054309 (2005).

20   Benne, B., Dobrijevic, M., Cavalié, T., Loison, J.-C. & Hickson, K. M. A photochemical model of Triton's atmosphere with an uncertainty propagation study. *Astron. Astrophys.* **667**, A169 (2022).

21   Cui, J. *et al.* Analysis of Titan's neutral upper atmosphere from Cassini Ion Neutral Mass Spectrometer measurements. *Icarus* **200**, 581-615 (2009).

22   Yelle, R. V. *et al.* Formation of NH_3 and CH_2NH in Titan's upper atmosphere. *Faraday Discuss.* **147**, 31-49 (2010).

23   Teanby, N. A. *et al.* Constraints on Titan's middle atmosphere ammonia abundance from Herschel/SPIRE sub-millimetre spectra. *Planet. Space Sci.* **75**, 136-147 (2013).

24   Nixon, C. A. *et al.* Upper limits for undetected trace species in the stratosphere of Titan. *Faraday Discuss.* **147**, 65-81 (2010).

25   Vuitton, V., Yelle, R. V. & McEwan, M. J. Ion chemistry and N-containing molecules in Titan's upper atmosphere. *Icarus* **191**, 722-742 (2007).

26   Teolis, B. D. *et al.* A revised sensitivity model for Cassini INMS: Results at Titan. *Space Sci. Rev.* **190**, 47-84 (2015).

27   Kaiser, R. I. Experimental investigation on the formation of carbon-bearing molecules in the interstellar medium via neutral−neutral reactions. *Chem. Rev.* **102**, 1309-1358 (2002).

28   Markwick, A. J., Millar, T. J. & Charnley, S. B. On the abundance gradients of organic molecules along the TMC-1 ridge. *Astrophys. J.* **535**, 256 (2000).

29   McElroy, D. *et al.* The UMIST database for astrochemistry 2012. *Astron. Astrophys.* **550**, A36 (2013).

30   Yang, Z. *et al.* Gas-phase formation of the resonantly stabilized 1-indenyl ($C_9H_7^{\bullet}$) radical in the interstellar medium. *Sci. Adv.* **9**, eadi5060 (2023).

31   Abplanalp, M. J. & Kaiser, R. I. Implications for extraterrestrial hydrocarbon chemistry: analysis of acetylene (C_2H_2) and D2-acetylene (C_2D_2) ices exposed to ionizing radiation via ultraviolet–visible spectroscopy, infrared spectroscopy, and reflectron time-of-flight mass spectrometry. *Astrophys. J.* **889**, 3 (2020).

32   Thrower, J. *et al.* Photon-and electron-stimulated desorption from laboratory models of interstellar ice grains. *J. Vac. Sci. Technol. A* **28**, 799-806 (2010).

33   Balucani, N. *et al.* Crossed beam reaction of cyano radicals with hydrocarbon molecules. III. Chemical dynamics of vinylcyanide (C_2H_3CN; X^1A') formation from reaction of CN ($X^2\Sigma^+$) with ethylene, C_2H_4 (X^1A_g). *J. Chem. Phys.* **113**, 8643-8655 (2000).

34   Kodama, S. Reactions of imidogen radicals. 6. Reactions of imidogen ($a^1\Delta$) with acetylene and unimolecular decompositions of C_2H_3N. *J. Phys. Chem.* **92**, 5019-5024 (1988).